Available online at www.sciencedirect.com
SCIENCE DIRECT®
International Journal of Mass Spectrometry 242 (2005) 87–94
International Journal of Mass Spectrometry
www.elsevier.com/locate/ijms

FT-ICR MS studies of ion-molecule reactions of Ru^+ and Os^+ with oxygen

Gerrit Marx[a], Achim Dretzke[b], Alexander Herlert[a,*], Werner Lauth[b], Hartmut Backe[b], Lutz Schweikhard[a]

[a] *Institut für Physik, Ernst-Moritz-Arndt-Universität Greifswald, D-17487 Greifswald, Germany*
[b] *Institut für Kernphysik, Johannes Gutenberg-Universität Mainz, D-55099 Mainz, Germany*

Received 21 July 2004; accepted 23 November 2004
Available online 7 January 2005

Abstract

The reactions of stored ruthenium and osmium cations with oxygen have been studied in a Fourier transform ion cyclotron resonance (FT-ICR) mass spectrometer. In case of osmium the reaction products OsO^+ and OsO_2^+ have been observed and corresponding reaction-rate constants have been determined. In addition, there is an unreactive fraction of Os^+ ions due to the presence of a slightly endothermic reacting ground state. Only the excited states react with oxygen. For ruthenium no spontaneous reaction with oxygen has been observed unless the cyclotron motion of Ru^+ was excited. The results are discussed with respect to a similar investigation in a Penning trap-TOF mass spectrometer [U. Rieth, A. Herlert, J.V. Kratz, L. Schweikhard, M. Vogel, C. Walther, Radiochim. Acta 90 (2002) 337] and with respect to possible future studies of ion-molecule reactions of the homologous super-heavy element 108 (hassium).

Keywords: Osmium; Ruthenium; Ion-molecule reaction; Penning trap

1. Introduction

The discovery of the heaviest elements [1] immediately raised the question of their properties. In particular, there is a strong interest in the chemical characterization with respect to their position in the periodic table of elements [2]. As the nuclear charge increases, strong relativistic effects on the electron configuration are expected [3,4], similar and in excess of those already observed, e.g., in the case of gas-phase ion chemistry of gold [5]. Experimental data and energy levels from Hartree-Fock calculations have been compared for the trans-actinides and their homologous elements in order to study the change in chemical behavior [6]. The results from gas-chromatographic experiments for the elements 104 (rutherfordium) and 105 (dubnium) showed deviations due to relativistic effects [7,8] whereas for the elements 106 (seaborgium) and 107 (bohrium) the expected position in the periodic table was confirmed [9,10]. Fully relativistic density functional calculations on the volatile group 8 tetroxides RuO_4, OsO_4 and HsO_4 predict a similarity of the element 108 (hassium) to its lighter homologues ruthenium and osmium [11]. Recently, the chemical separation and characterization of hassium has been performed with a new gas-chromatographic separation system [12], and the oxidation of seven Hs atoms to HsO_4 could be found and compared to the production of OsO_4 confirming the predicted chemical behavior of element 108 [13].

In addition to the aqueous and gas-chromatographic experiments, the use of the ion trapping device SHIPTRAP [14] is planned for the investigation of superheavy elements. This device is a Penning-trap apparatus located at SHIP, a kinematic separator for reaction recoil particles from thin targets. For the production of superheavy elements, the targets are irradiated by beams of heavy ions from the linear accelerator UNILAC at GSI [15]. After their flight through SHIP the recoil ions are stopped in a “gas cell”, a chamber filled with

* Corresponding author. Present address: CERN, Physics Department, CH-1211 Geneva 23, Switzerland.
E-mail address: alexander.herlert@cern.ch (A. Herlert).

1387-3806/$ – see front matter © 2004 Elsevier B.V. All rights reserved.
doi:10.1016/j.ijms.2004.11.014

nobel gas, bunched and thermalized in a radiofrequency trapping system and finally transferred into a Penning trap where they are captured in flight. While the ions are stored their reaction kinematics with respect to given gases may be studied. The variable storage duration will allow the investigation of short- as well as long-lived trans-actinides, including those with a half-life $T < 100$ ms which are not accessible to gas-chromatographic methods. As a first test of the future gas-phase ion-molecule reactions of the heaviest elements at SHIPTRAP, the oxidation of ruthenium and osmium has been investigated recently [16] at the ClusterTrap, a Penning trap-TOF mass spectrometer [17]. The reaction of osmium up to the dioxide OsO_2^+ was observed and the osmium and osmiumoxide reaction rates were determined [16], although earlier bond-energy values infer a slightly endothermic reaction with oxygen [18]. In addition, the observation of a spontaneous reaction of ruthenium was observed in contradiction to a previously reported endothermic behavior [19] and thus left the results in a status which asked for further investigations. In the following, an independent experiment on the ion-molecule reactions of Ru^+ and Os^+ with oxygen is presented, where FT-ICR mass spectrometry was applied.

2. Experimental setup and procedure

The experiments were performed with a commercial FT-ICR mass spectrometer (EXTREL FT/MS 2001-DX), which is equipped with a 2.7-T superconducting magnet and a "dual-cell" trap configuration, i.e., two cubic ICR cells, each of two-inch size. Fig. 1(a) shows a schematic overview of the experimental setup. For the present experiments only the source cell has been used. A scheme of the experimental sequence is shown in Fig. 1(b): Before the production and capturing of the ions the cell was emptied by pulsing the trapping plate potential to −10 V. The osmium and ruthenium ions were produced by laser ablation from a corresponding target with a CO_2 laser at a wavelength of 10.6 μm. These targets consisted of copper plates where osmium and ruthenium had been electrolytically deposited on [16]. They were mounted on the automatic solids-probe of the spectrometer. The target was set to about 5 mm distance from the trapping plate of the cell and rotated to bring new osmium or ruthenium material to the position of the laser pulse focus on the probe. Both trapping plates may be set to a variable potential of 1 to 10 V (with respect to the excite/detect plates which were on ground potential). In general, a trapping potential of $U_0 = 1$ V has been applied. For capturing, the endcap plate potential is set to 0 V to allow the ions to drift into the source cell. 80 μs after the laser pulse, i.e., just before the ions can leave the cell, the trapping plate potential is reset to 1 V. In addition to the laser ablation from the target, ions can be produced by ionization of gas particles in the cell volume by 70-eV electrons from an electron gun. The electron beam is applied for about 200 ms and since the ions are produced inside the ion trap the potentials need not to be changed during the electron bombardment.

The stored ruthenium or osmium ions were subjected to the oxygen gas, which is introduced to the cell through a leak valve at a pressure range of 4×10^{-8} mbar to 2×10^{-6} mbar (the pressure in the cell volume was determined as described in the Appendix). In addition to the reaction gas, a colli-

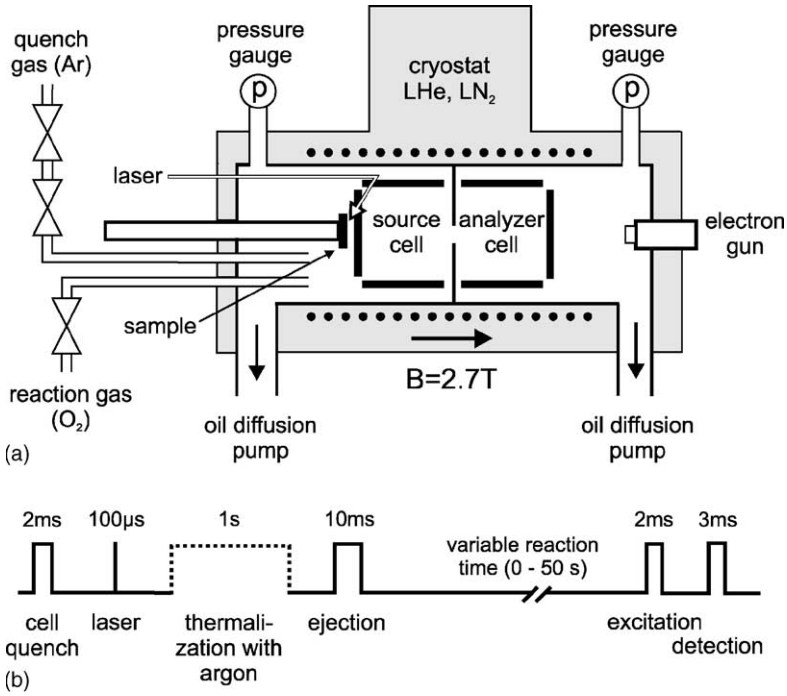

Fig. 1. (a) Overview of the experimental setup. (b) Experimental sequence. The thermalization with argon (dashed line) was not applied in all measurements.

sion gas (argon) may be pulsed into the cell region. With two sequentially mounted valves a pulse of approximately 1×10^{-4} mbar is applied for a one-second collision period to quench electronically excited states to the ground state of the ions and to bring the ion ensemble in the trap to room temperature. The reaction period was varied between 0 and 50 s. Starting conditions were defined by the removal of all ions that had already reacted with oxygen by resonant radial ejection. After a defined delay, i.e., a reaction period, all ions stored in the cell were detected by standard FT-ICR mass analysis: A dipolar excitation of the cyclotron motion of the ions was applied with a frequency sweep at a rate of 1.2 kHz/μs for 2.14 ms. The ion signal was recorded for about 3 ms with a sample rate of 5.3 MHz for a transient length of 16K data points. The resolving power was about 1400 for Ru^+ and 700 for Os^+.

3. Results

3.1. Reaction of Ru^+ with oxygen

The ruthenium cations are stored in the source cell and exposed to oxygen at a fixed pressure for a variable reaction time ($10\,\mu s < \Delta t < 50\,s$). After the reaction time the remaining precursor ions as well as the metal-oxide and metal-dioxide product ions are detected. Fig. 2(a) shows a typical mass spectrum as recorded after a reaction period of 50 s at a pressure $p = 3.0 \times 10^{-7}$ mbar. The reaction of ruthenium ions with oxygen

$$Ru^+ + O_2 \rightarrow RuO^+ + O^\bullet \quad (1)$$

is endothermic with $D(Ru^+–O) = 3.81(5)$ eV [19]. Thus, as expected, no oxidation process was observed (see Fig. 2(a)). The situation changes if the kinetic energy of the ions is increased. Fig. 2(b) shows a mass spectrum that demonstrates the formation of RuO^+ after ICR excitation (frequency sweep with a rate of 4 Hz/μs for a range of 33 kHz) of all isotopes with the exception of $^{96}Ru^+$. An increase of the radius of the cyclotron motion up to 2.4 cm corresponds to an increase of the kinetic energy of the ions in the ICR cell of up to 1.2 keV. Thus, the Ru^+ ions may overcome the endothermic barrier and form RuO^+. Since the manipulation of the ion motion and therefore of the kinetic energy is mass selective, only one single isotope may be excited for the reaction with oxygen. As an example, Fig. 2(c) shows the oxidation of $^{102}Ru^+$ as the only isotope of the ensemble from ^{96}Ru to ^{104}Ru (excitation frequency sweep range 5 kHz). In general, the threshold for an endothermic reaction can be determined by use of a FT-ICR mass spectrometer [20] similar as with a guided ion beam mass spectrometer in the case of the reaction of Ru^+ with oxygen [19]. However, the absolute excitation amplitude was not available in the present study.

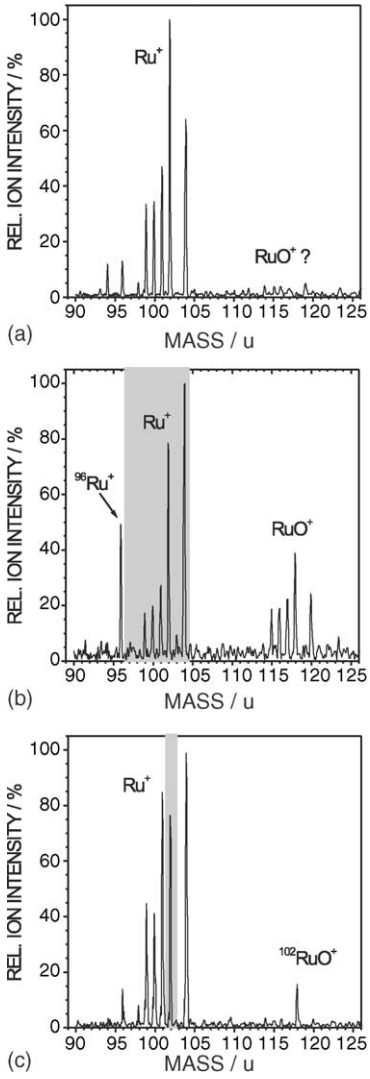

Fig. 2. (a) FT-ICR mass spectra after the reaction of Ru^+ with oxygen at a pressure $p = 3.0 \times 10^{-7}$ mbar for $t = 50$ s. (b) FT-ICR mass spectra after the reaction of Ru^+ with oxygen at a pressure $p = 4.4 \times 10^{-6}$ mbar for $t = 5$ s. The ruthenium isotopes that are excited with a dipolar rf-excitation prior to the reaction period are marked with a shaded area. Only ^{96}Ru is not excited. (c) FT-ICR mass spectra after the reaction of Ru^+ with oxygen at a pressure $p = 5.7 \times 10^{-6}$ mbar for $t = 5$ s. Only one isotope, ^{102}Ru, has been excited with a dipolar rf-excitation (indicated with the shaded area).

3.2. Reaction of osmium ions with oxygen

A spontaneous oxidation of osmium ions has been observed in a previous investigation [16], although an endothermic behavior is expected [18]. In the present experiment a reaction of osmium ions with oxygen was observed, too. As an example, Fig. 3 shows FT-ICR mass spectra with the relative ion intensities for the reaction of Os^+ with oxygen at a pressure $p = 2.3 \times 10^{-7}$ mbar for different reaction periods. The mass spectra show the production of the monoxide and dioxide which can be clearly identified with the characteristic isotopic pattern of osmium. No higher oxides have been observed. From the relative abundances of Os^+, OsO^+ and

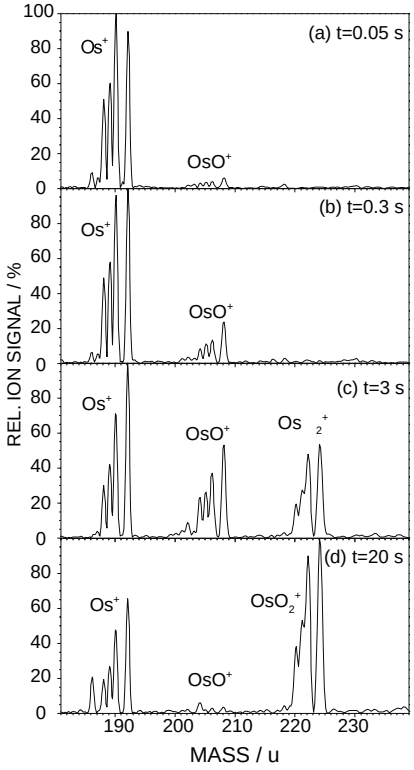

Fig. 3. FT-ICR mass spectra after the reaction of Os^+ with oxygen at a pressure $p = 2.3 \times 10^{-7}$ mbar for $t = 0.05$, 0.3, 3, and 20 s.

OsO_2^+ the reaction kinetics can be derived. As an example, the relative ion intensities of the osmium ions (empty circles), the monoxide ions (filled circles) and the dioxide ions (filled triangles) are shown in Fig. 4 as a function of the reaction period for a pressure $p = 5.8 \times 10^{-7}$ mbar. The Os^+ signal shows an exponential decrease. The monoxide-ion signal increases at some 10 ms to a maximum at about 600 ms and disappears almost completely for large reaction times. This decrease of the OsO^+ signal is accompanied by the formation of osmium-dioxide ions. The solid lines represent fits to the

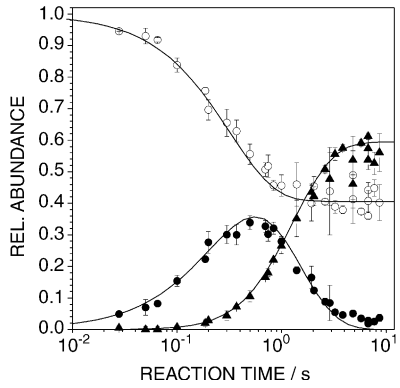

Fig. 4. Relative abundance of Os^+ (empty circles), OsO^+ (filled circles), and OsO_2^+ (filled triangles) as a function of the reaction time t. The solid lines represent the result of a simultaneous fit of the rate equations to the data. The pressure was $p = 5.8 \times 10^{-7}$ mbar and the trapping potential $U_0 = 10$ V.

measured data as discussed below. Obviously, the reaction is at least composed of two sequential oxidation steps:

$$Os^+ + O_2 \rightarrow OsO^+ + O^\bullet, \quad \text{with rate constant } k_1 \tag{2}$$

$$OsO^+ + O_2 \rightarrow OsO_2^+ + O^\bullet, \quad \text{with rate constant } k_2 \tag{3}$$

In addition to the reactions observed, a fraction of the Os^+ ions does not react to OsO^+. The solution of the differential equations of sequential reactions (or decays) is a set of exponential functions, which describe the intensities of the precursor and the products. In the present case:

$$N_0(t) = n_0 + (1 - n_0)\mathrm{e}^{-c_1 t} \tag{4}$$

$$N_1(t) = (1 - n_0)\frac{c_1}{c_2 - c_1}(\mathrm{e}^{-c_1 t} - \mathrm{e}^{-c_2 t}) \tag{5}$$

$$N_2(t) = (1 - n_0)\left[1 + \frac{1}{c_2 - c_1}(c_1 \mathrm{e}^{-c_2 t} - c_2 \mathrm{e}^{-c_1 t})\right] \tag{6}$$

where N_i represent the relative abundance of osmium, osmium-monoxide and osmium-dioxide ions and n_0 is the fraction of osmium ions that do not react with oxygen. The pressure-dependent rate constants c_1 and c_2 as well as the fraction n_0 were obtained from a simultaneous least-square fit of Eqs. (4)–(6) to the data. From these fit parameters the reaction rate constants k_1 and k_2 are calculated by

$$k_i = c_i \frac{k_B T}{p}, \quad i = 1, 2 \tag{7}$$

where $T = 300$ K is assumed for the ambient temperature. As indicated by the solid lines in Fig. 4 the data are well fitted by the equations. The osmium reaction has been investigated for five different oxygen pressures. These measurements yield values for the reaction rates k_1 and k_2 as shown in Fig. 5(a) (filled and empty circles, respectively). The deviations are due to day-to-day fluctuations. The mean values are $\langle k_1 \rangle = (1.5 \pm 0.1) \times 10^{-10}$ cm^3 molecule^{-1} s^{-1} and $\langle k_2 \rangle = (5.0 \pm 0.3) \times 10^{-11}$ cm^3 molecule^{-1} s^{-1} as indicated in Fig. 5(a) by the shaded areas. No dependence of the rate constants k_1 and k_2 on the pressure p is observed.

To investigate the origin of Os^+ ions which do not react, the fraction n_0 is plotted as a function of the oxygen pressure p in Fig. 5(b) (filled circles). The mean value (dashed line) is given by $\langle n_0 \rangle = 0.35(2)$. No dependence on the pressure is observed where the deviations to the mean value are correlated to the day-to-day fluctuations of the measured rate constants. The data was also analyzed for each isotope separately. For the isotopes ^{188}Os, ^{189}Os, ^{190}Os, and ^{192}Os the corresponding rate constants and fractions were determined and no isotope dependence was observed.

In addition, the reaction was investigated as a function of the trapping potential. The maximum kinetic energy in the axial harmonic motion of the ions in the electrostatic quadrupole potential of the ICR cell depends on the trapping potential U_0 which is applied between the trapping plates and the ring electrode plates. The rate constants k_1 and k_2 have been measured as a function of U_0. The result is shown in Fig. 6(a) with

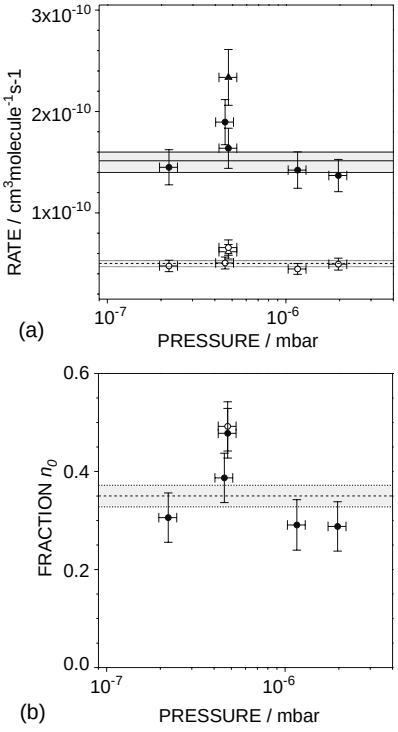

Fig. 5. (a) Reaction rates k_1 (filled circles) of Os^+ and k_2 (empty circles) of OsO^+ with oxygen as a function of the oxygen pressure in the ICR cell. As a comparison the result of a measurement with argon quench is shown with a triangle as symbol. The mean values are given with a solid and dashed line, respectively, where the uncertainties are indicated by the shaded areas. (b) Fraction n_0 as a function of the oxygen pressure in the ICR-cell. The dashed line indicates the mean value.

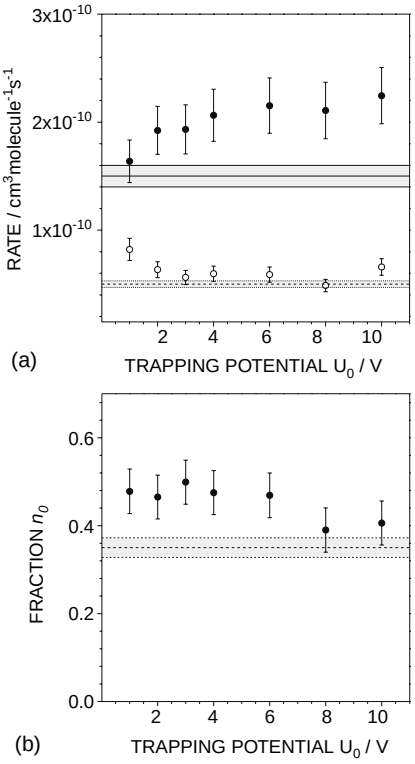

Fig. 6. (a) Reaction rates k_1 (filled symbols) and k_2 (empty symbols), and (b) fraction n_0 as a function of the trapping potential U_0 applied between ring electrode plates and endcap plates. For comparison the solid and dashed lines give the mean values as determined in Fig. 5 for a different series of measurement (on different days) at $U_0 = 1$ V.

filled and empty symbols, respectively. For comparison the mean values for k_1 and k_2 as determined above ($U_0 = 1$ V) are indicated. While for k_2 no significant change is observed, the rate k_1 seems to increase for larger values of U_0. The dependence of the fraction n_0 on the trapping potential U_0 is shown in Fig. 6(b), where a slight decrease for larger trapping potentials is observed.

As discussed below, the observation of a non-reacting fraction n_0 indicates that the reactions are due to excited states. With the application of an argon gas pulse before the reaction a quenching of the excited states has been tried. No significant change in the measured rate constants k_1 and k_2 as well as the observed fraction n_0 has been found within the pressure regime investigated ($p < 2.0 \times 10^{-6}$ mbar). As an example the result from one measurement with argon-quenching is plotted in Fig. 5(a) with filled and empty triangles and in Fig. 5(b) with an empty circle. Only in case of the rate k_1 the deviation seems larger than expected from a statistical fluctuation. However, during the measurements variations were observed, e.g., on a day-to-day basis (with and without quenching).

4. Discussion

The recent study of the reaction of ruthenium ions with oxygen [16] showed a reaction of Ru^+ to the monoxide and even to the dioxide although the reaction is known to be endothermic [19]. The present FT-ICR MS investigation confirms the endothermicity of the reactions. Only an increase of the kinetic energy of specific ruthenium isotopes results in the corresponding reaction to RuO^+. Note that in the previous work [16] a quadrupolar excitation of all ions including the oxides had been applied to center the ions [21] and thus to avoid ion loss. For convenience oxygen had been used both as reaction gas and as buffer gas for axialization. With the application of the quadrupolar excitation the kinetic energy of the ions probably has been excited similar to the case of dipolar excitation in the present FT-ICR study where a reaction with oxygen was induced. Since all ion species, i.e., Ru^+, RuO^+ and $RuO_2{}^+$, had been centered by quadrupolar excitation even a reaction to the dioxide occurred. In contrast, in the present study only the Ru^+ ions were excited and thus no higher oxides of ruthenium were produced.

With respect to the possible influence of the quadrupolar excitation on the osmium reaction rates, the situation is somewhat different. The rates reported earlier $k_1' = (2.6 \pm 0.3) \times 10^{-12}\,\mathrm{cm^3\,molecule^{-1}\,s^{-1}}$ and $k_2' = (9.4 \pm 4.0) \times 10^{-12}\,\mathrm{cm^3\,molecule^{-1}\,s^{-1}}$ [16] are about 100 and 5 times smaller, respectively, than the present FT-ICR rates. Especially the first reaction to the monoxide deviates significantly. The difference is also obvious from the relative abundance

Table 1
Electronic states of ruthenium and osmium ions and their population from a Maxwell–Boltzmann distribution (data taken from [25,26])

Ion	State	Electron configuration	J	Energy (eV)	Population (%)				
					300 K	700 K	1500 K	3000 K	7000 K
Ru^+	$4d^7$	$a\,^4F$	9/2	0.000	99.95	96.23	79.27	58.75	36.10
			7/2	0.189	0.05	3.36	14.71	22.64	21.12
			5/2	0.309	$\ll 0.01$	0.34	4.35	10.66	12.97
			3/2	0.385		0.07	1.61	5.30	7.63
	$4d^7$	$a\,^4P$	5/2	1.024		$\ll 0.01$	0.02	0.67	3.97
			3/2	1.051			0.01	0.40	2.53
			1/2	1.162			$\ll 0.01$	0.13	1.05
	$4d^6(^5D)5s$	$a\,^6D$	9/2	1.135			0.01	0.73	5.50
			7/2	1.258			$\ll 0.01$	0.36	3.59
			5/2	1.345			$\ll 0.01$	0.19	2.33
			3/2	1.401				0.10	1.41
			1/2	1.439				0.04	0.66
Os^+	$5d^6(^5D)6s$	^6D	9/2	0.000	100.00	99.93	95.98	77.32	42.27
			7/2	0.445		0.05	2.45	11.04	16.16
			5/2	0.487		0.02	1.33	7.05	11.31
			3/2	0.693		$\ll 0.01$	0.18	2.12	5.36
			1/2	0.823			0.03	0.64	2.16
	$5d^56s^2$	^6S	5/2	0.978			0.03	1.05	5.01
	$5d^5(^5D)6s$	^4D	7/2	1.421			$\ll 0.01$	0.25	3.21
			5/2	1.445				0.17	2.31
			3/2	1.629				0.06	1.14

of produced monoxides. In [16] the maximum relative abundance is only a few percent whereas here the maximum value reaches about 40% OsO^+. In the earlier study the decrease of the Os^+ cations took place in the same time range as the creation of the dioxide ions. In the present investigation the relative abundances clearly show different time domains for the decay of Os^+ and the build up of $OsO_2{}^+$.

While the monoxide ions OsO^+ react completely to the dioxide ions, a large fraction of original precursor ions, Os^+, does not react at all. This indicates the existence of states with different reaction rates or endothermic behavior. Note that the ground state does not necessarily have the lowest reaction rate [22]. For example, in the ion-molecule reaction of Fe^+ with NO some excited states of Fe^+ do not react in contrast to the ground state [23]. Excited electronic states of ions may be generated in laser ablation from a target [24] as applied in the present investigation.

In a FT-ICR study of gas-phase ion chemistry of osmium tetroxide and its fragment ions by Irikura and Beauchamp [18], the bond energies of OsO^+ and $OsO_2{}^+$ were determined. Although the direct reaction of Os^+ with oxygen was not investigated, the bond energies were derived from thermochemical quantities obtained from several other observed reactions, e.g. $OsO_n{}^+ + H_2 \rightarrow OsO_{n-1}{}^+ + H_2O$ ($n = 1-3$). The calculated bond energies are $D(Os^+{-}O) = 4.34(52)$ eV and $D(OsO^+{-}O) = 4.55(52)$ eV, which are smaller than the bond energy of the oxygen molecule $D(O{-}O) = 5.12$ eV [19]. Therefore, a slightly endothermic behavior is expected.

The observed reaction of Os^+ is thus probably due to excited states that have been produced during the creation of the ions by laser ablation from the target. Table 1 lists excited states of Ru^+ and Os^+ and their population for several different temperatures. In the case of osmium the population of the excited states at $T = 7000$ K is similar to the fraction of ions that have reacted with oxygen. The lowest excited state with $E = 0.445$ eV lies well within the energy difference $D(O{-}O) - D(Os^+{-}O) = 0.78(52)$ eV, i.e., allows a reaction to the monoxide. In the case of the ruthenium ions the energy of the populated excited states up to $T = 7000$ K is not sufficient to overcome the energy difference $D(O{-}O) - D(Ru^+{-}O) = 1.31(5)$ eV to form RuO^+. This is in agreement with the experimental results where only kinetically excited ions react with oxygen.

5. Summary and conclusion

For ruthenium an endothermic reaction with oxygen has been confirmed and the recently observed reaction to RuO^+ [16] can be explained with the reported quadrupolar excitation that has been applied during the reaction period to reduce ion loss for large reaction times. The quadrupolar excitation in Ref. [16] might have led to an increase of the kinetic energy of the ions and thus to a reaction with oxygen. A similar effect on the osmium reaction kinetics cannot be excluded and may have influenced the results.

In the case of osmium ions a reaction with oxygen has been observed and the rate constants k_1 for the reaction $Os^+ + O_2 \rightarrow OsO^+ + O^\bullet$ and k_2 for the reaction $OsO^+ + O_2 \rightarrow OsO_2{}^+ + O^\bullet$ have been determined: $k_1 = (1.5 \pm 0.1) \times 10^{-10}$ cm^3 molecule^{-1} s^{-1} and $k_2 = (5.0 \pm 0.3) \times 10^{-11}$ cm^3 molecule^{-1} s^{-1} (only the statistical uncer-

tainties are given). No higher oxides have been observed. A fraction of unreactive osmium cations is explained with a non-reactive ground state of Os^+. The comparison to the previous investigation [16] shows a deviation in the rates of about two orders of magnitude, possibly due to kinetically excited ions rather than excited states as in the present study. The application of gas pulses to quench the reactive excited states by collisions with argon atoms showed only minor changes of the observed fraction or the reaction rates. Further investigations of the quenching process are necessary and other nobel gases might be more efficient than argon.

The endothermic behavior of ruthenium and osmium in the reaction with oxygen as well as the measured reaction rates for the excited states of Os^+ lead to the same conclusion as in Ref. [16] with respect to reactions of the homologous element hassium: The partial pressures of oxygen that allow long reaction times without significant ion loss might be too low to perform ion chemistry for the superheavy elements in an ion trap. However, for long lived isotopes like ^{269}Hs with about 10 s half-life ion-molecule reactions in an ICR cell are still to be considered, especially with respect to reaction dynamics which can be monitored with FT-ICR mass analysis without removing the ions from the trap. Other exothermic reactions should be studied and compared between the homologous elements. For example the bond energy of N_2O is smaller than the bond energies of the osmium oxides and a recent investigation of gas-phase oxidation of Os^+ with nitrous oxide clearly showed the exothermic production of osmium oxides up to the tetroxide $OsO_4{}^+$ [27]. In addition, reactions in gas cells, which are used to stop the superheavy ions after creation, have the advantage of higher partial pressures of the reactive gases which are mixed with the buffer gas (usually a noble gas like helium or argon) [28] and the reaction products may be transferred to the Penning trap for mass analysis.

Acknowledgements

This work has been supported by the Fonds der Chemischen Industrie, the Bundesministerium für Bildung und Forschung under Contract No. 06 MZ 959 I, and the GSI Hochschulprogramm (MZ-BAC and GF-SCH). We thank Ulrich Rieth for preparing the osmium and ruthenium targets. We also thank the unknown reviewers for their valuable advice.

Appendix. Calibration of pressure gauge

The pressure in the ion cell cannot be measured directly and therefore needs to be calibrated for the ion-molecule reaction measurements. The calibration was performed by use of the well-known reaction

$$CH_4{}^+ + CH_4 \rightarrow CH_5{}^+ + CH_3 \tag{8}$$

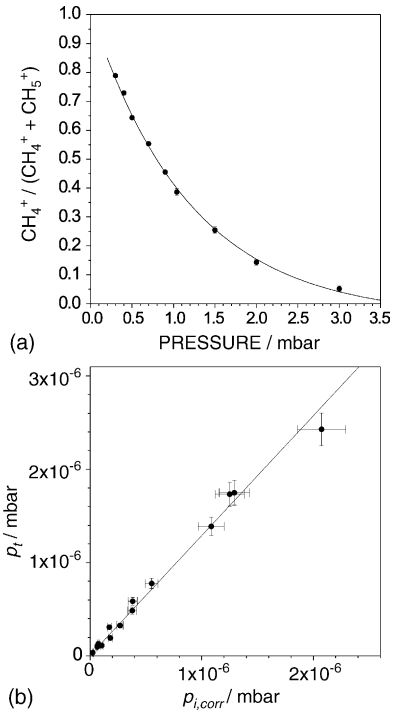

Fig. 7. (a) Relative abundance of $CH_4{}^+$ as a function of the reaction time at a methane pressure of 3.5×10^{-8} mbar. In this example the rate constant for the reaction of methane $CH_4{}^+$ to $CH_5{}^+$ is $c = 0.96(2)\,s^{-1}$. (b) Calibration of the pressure gauge: "true pressure" as a function of the corrected pressure readout $p_{i,corr}$, which has been adjusted with the corresponding empirical gas-correction factor R_g (for details see Appendix).

which has a reaction constant of $k_0 = (1.13 \pm 0.08) \times 10^{-9}\,cm^3\,molecule^{-1}\,s^{-1}$ (at $T = 300$ K) (mean value from [29]). The methane ions were created in the source cell by electron impact ionization as described in Section 2. For a given pressure readout p_i of a Bayard–Alpert ionization gauge the ratio

$$R = \frac{[CH_4{}^+]}{[CH_4{}^+] + [CH_5{}^+]} \tag{9}$$

was measured as a function of the reaction period t as shown in Fig. 7(a). With an exponential fit to the data, $R(t) = a\exp(-ct)$, the actual pressure in the ICR cell p_t was determined in analogy to Eq. (7)

$$p_t = c\frac{k_{BT}}{k_0} \tag{10}$$

In addition, the pressure readout needs to be adjusted for the use of methane since the gauge is normalized to nitrogen:

$$p_{i,corr} = p_i R_g \tag{11}$$

where the correction factors $R_g(\text{methane}) = 0.62(2)$ and $R_g(\text{oxygen}) = 1.15(2)$ [30] have been applied for the determination of the oxygen pressure in the source cell. In Fig. 7(b) the resulting linear correlation between the corrected pressure readout $p_{i,corr}$ and the determined actual pressure p_t is shown.

References

[1] S. Hofmann, G. Münzenberg, Rev. Mod. Phys. 72 (2000) 733.
[2] A. Türler, Eur. Phys. J. A 15 (2002) 271.
[3] B. Fricke, W. Greiner, Phys. Lett. B 30 (1969) 317.
[4] V.G. Pershina, Chem. Rev. 96 (1996) 1977.
[5] H. Schwarz, Angew. Chem. Int. Ed. 42 (2003) 4442.
[6] W.C. Martin, J. Sugar, Phys. Rev. A 53 (1996) 1911.
[7] M. Schädel, Radiochim. Acta 70/71 (1996) 207.
[8] D.C. Hoffman, Radiochim. Acta 72 (1996) 1.
[9] M. Schädel, et al., Nature 388 (1997) 55.
[10] R. Eichler, et al., Nature 407 (2000) 63.
[11] V. Pershina, T. Bastug, B. Fricke, S. Varga, J. Chem. Phys. 115 (2001) 792.
[12] Ch.E. Düllmann, B. Eichler, R. Eichler, H.W. Gäggeler, D.T. Jost, D. Piguet, A. Türler, Nucl. Instr. Methods A 479 (2002) 631.
[13] Ch.E. Düllmann, et al., Nature 418 (2002) 859.
[14] G. Marx, et al., Hyperfine Int. 146/147 (2003) 245.
[15] G. Münzenberg, W. Faust, S. Hofmann, P. Armbruster, K. Güttner, H. Ewald, Nucl. Instr. Methods 161 (1979) 65.
[16] U. Rieth, A. Herlert, J.V. Kratz, L. Schweikhard, M. Vogel, C. Walther, Radiochim. Acta 90 (2002) 337.
[17] L. Schweikhard, K. Hansen, A. Herlert, G. Marx, M. Vogel, Eur. Phys. J. D 24 (2003) 137.
[18] K.K. Irikura, J.L. Beauchamp, J. Am. Chem. Soc. 111 (1989) 75.
[19] Y.-M. Chen, P.B. Armentrout, J. Chem. Phys. 103 (1995) 618.
[20] M. Beyer, V.E. Bondybey, Rapid Commun. Mass Spectrom. 11 (1997) 1588.
[21] G. Savard, St. Becker, G. Bollen, H.-J. Kluge, R.B. Moore, L. Schweikhard, H. Stolzenberg, U. Wiess, Phys. Lett. A 158 (1991) 247.
[22] P.B. Armentrout, Science 251 (1991) 175.
[23] J.V.B. Oriedo, D.H. Russell, J. Am. Chem. Soc. 115 (1993) 8376.
[24] H. Kang, J.L. Beauchamp, J. Phys. Chem. 89 (1985) 3364.
[25] A.G. Shenstone, W.F. Meggers, J. Res. Natl. Bur. Stand. 61 (1958) 373.
[26] Th.A.M. van Kleef, P.F.A. Klinkenberg, Physica 27 (1961) 83.
[27] V.V. Lavrov, V. Blagojevic, G.K. Koyanagi, G. Orlova, D.K. Bohme, J. Phys. Chem. A 108 (2004) 5610.
[28] A. Dretzke, H. Backe, G. Kube, W. Lauth, W. Ludolphs, A. Morbach, M. Sewtz, Hyperfine Int. 132 (2001) 501.
[29] Y. Ikezoe, S. Matsuoka, M. Takebe, A. Viggiano (Eds.), Gas Phase Ion-Molecule Reaction Rate Constants Through 1986, The Mass Spectroscopy Society of Japan, Tokyo, 1987 (and references therein).
[30] J.E. Bartmess, R.M. Georgiadis, Vacuum 33 (1983) 149.